Journal of the European Ceramic Society 18 (1998) 1245–1250

PII: S0955-2219(98)00049-1
0955-2219/98/$—see front matter

# Hydrothermal Synthesis of Calcium Deficient Hydroxyapatites with Controlled Size and Homogeneous Morphology

M. Andrés-Vergés,* C. Fernández-González and M. Martínez-Gallego

Departamento Química Inorgánica, Universidad de Extremadura, Avda. Elvas s/n. 06071-Badajoz, Spain

***Abstract***

*Preparation of needle-like calcium deficient hydroxyapatites from hydrothermal decomposition of the calcium chelate Ca–EDTA in the presence of $PO_4^{3-}$ groups is reported. Different conditions relative to reactant concentrations: Ca $(NO_3)_2$=0·01–0·3 mol $\times dm^{-3}$ (M), $(NH_4)_2HPO_4/Ca$ $(NO_3)_2$=6/10, $Na_2$-EDTA/Ca $(NO_3)_2$ (R)=1-1·5; temperature=150–220°C and pH=8–12, have been tested in order to ascertain their influence on the stoichiometric degree and morphology. For Ca $(NO_3)_2$ 0·05 M, R=1, pH=11 and temperature 200°C, well elongated particles were obtained. On the other hand, the stoichiometric degree expressed as Ca/P ratio resulted in being dramatically affected by variations in pH, ranging from 1·45 for pH=8 up to 1·63 for pH=11.*

## 1 Introduction

Calcium phosphates are an important class of compounds principally because of their biological relationships. One of these compounds, the hydroxyapatite $Ca_{10}(PO_4)_6(OH)_2$ (HA), is the structural prototype and a lot of attention has been devoted to it many years ago. An important part of this attention is related to the experimental procedures for obtaining HA and related compounds. So, wet precipitation,[1–4] hydrothermal,[5–8] hydrolysis of salts,[9] solid state,[10] sputtering,[11] methods etc. have been reported. In spite of the large amount of procedures, only a few have been devoted to preparing apatitic compounds with controlled morphology.[8,12] The attention of apatitic compounds transcends the biological area because of its unique surface-structure consisting of calcium, phosphate and hydroxide ions, so applications as catalyst[13,14] and ionic exchanger[15,16] have been reported as well. More recently, the electrical properties of hydroxyapatites have been studied because of their potential applications as gas sensors[17] and proton conductors at high temperatures.[18,19] When the proton conductors suitable for fuel cells are reviewed,[20] it can be concluded that there is a need to develop good materials in the temperature range 200–400°C, because most proton conductors are unstable at temperatures greater than 150°C and possess low electrical conductivity. Calcium deficient hydroxyapatites present structural characteristics which might be suitable for a good electrical conductivity at temperatures below 400°C.

According to Joris and Amberg,[21] the calcium deficient hydroxyapatites can be represented by the models I and II, depending on the Ca/P ratio:

$$Ca_{10-x}(HPO_4)_x(PO_4)_{6-x}(OH)_{2-x}(H_2O)_x \quad x < 1 \tag{I}$$

$$Ca_{9-x}(HPO_4)_{1+2x}(PO_4)_{5-2x}(OH).H_2O \quad x < 1 \tag{II}$$

It has been showed, that $H_2O$ molecules are located on the places corresponding to the missing $OH^-$ groups, and they are hydrogen bonded to the nearest $PO_4^{3-}$ groups. This class of compounds present lower stability than stoichiometric ones, and above 200°C, the $HPO_4^{2-}$groups begin to transform into $P_2O_7^{4-}$. The condensation process takes place along a wide interval of temperature, and only above 300°C can be considered almost finished. Because of the presence of $HPO_4^{2-}$charge carriers and the high mobility of them in this

*To whom correspondence should be addressed.

interval of temperature, we think that such materials might be suitable for testing protonic conductivities.

In order to study the contributions of the size, morphology and composition to the ionic conductivity, in the present work we report the synthesis of needle-like calcium deficient hydroxyapatites belonging to both types of model. With this aim, a hydrothermal procedure based in the decomposition of calcium chelate Ca–EDTA in the presence of $PO_4^{3-}$groups, at pH = 8–12 and temperatures ranging between 150 and 220°C has been followed. The influence that several parameters as concentrations of reactants, pH, temperature and aging time have on some of the physical and chemical characteristics of the hydroxyapatites is shown.

## 2 Experimental

All chemicals were analytical reagent grade and sample solutions of Ca/P ratio equal to 1·67 (stoichiometric ratio of HA) were prepared in all cases as follow:

### 2.1 Procedure

First, it was proved that the order of reactants mixing had a strong influence on the synthesis of hydroxyapatites. So, when a $(NH_4)_2HPO_4$ solution is added on a 1:1 mixed solution of $Na_2$–EDTA and $Ca(NO_3)_2$ ($R=1$), a white precipitate of a hydroxyapatite precursor immediately appears even for the lower studied calcium concentrations. Therefore, all the solutions were prepared in an opposite manner to previously mentioned. On the other hand, for pH higher than 11 the value of $R$ was increased to 1·1 in order to prevent the formation of precipitate. The general procedure followed was: 100 ml of a mixed solution of calcium nitrate ($2\times10^{-2}$-$6\cdot10^{-1}$ M) and ethylenediaminetetracetic acid disodium salt, $Na_2$–EDTA ($2\times10^{-2}$-$8\times10^{-1}$ M) ($R$ was varied between 1 and 1·5) was added to 100 ml of an diammonium hydrogen phosphate ($1\cdot2\times10^{-2}$–$3\cdot6\times10^{-1}$ M) solution. The pH of both solutions was adjusted to 8–12 by adding $NH_3$ solution. The final solution was put in a teflon vessel and heated in a Parr reactor at temperatures ranging between 150 and 220°C.

The synthesis of hydroxyapatites is based on the thermal decomposition of calcium chelate Ca–EDTA in presence of $(PO_4)^{3-}$ groups

$$Ca - EDTA = Ca^{2+} + EDTA^{2-} \quad (1)$$

$$10Ca^{2+} + 6PO_4^{3-} + 2OH^- = Ca_{10}(PO_4)_6(OH)_2 \quad (2)$$

Therefore, factors affecting the equilibrium of both (1) and (2) must be considered in order to achieve well developed microcrystals. With this aim, a large reaction time $t$ was selected (standard time $t=1$ h), and the influence of temperature, pH, reactant concentrations and aging time were considered.

The equilibrium (1) is critically dependent on the temperature in such a manner, that above 220°C, appreciable decomposition of $EDTA^{2-}$ has been observed, which produces carbonate apatites. Therefore, only temperatures below 220°C were selected. Standard conditions for obtaining hydroxyapatite were: Ca $(NO_3)_2=0\cdot05$M, $R=1$, $(NH_4)_2HPO_4/Ca(NO_3)_2=6/10$ and pH = 11. The system was maintained at 200°C for 1 h. The precipitates formed were filtered by a membrane filter, washed and dried at 90°C for 12 h.

### 2.2 Characterisation

The produced crystalline phases were identified by X-ray diffraction technique (XRD), infrared absorption spectroscopy (IR) and scanning electron microscopy (SEM). Because of the elongated morphology of the particles, the XRD patterns have been recorded as oriented and non-oriented aggregate films. The chemical compositions were determined by atomic absorption spectroscopy (calcium) and spectrophotometric method (phosphorus).

## 3 Results and Discussion

### 3.1 Standard conditions

The SEM of colloidal hydroxyapatites crystals synthesised from the standard conditions is given in Fig. 1(b). The XRD patterns showed characteristic and well defined hydroxyapatite diffraction lines. From both oriented and non-oriented aggregate film diffractograms, a noteworthy intensity change is observed for (h00) and (hkl) diffraction lines in such a manner that several of them as (112) and (202) disappear in the oriented XRD. This can be seen from the patterns recorded for $2\theta$ values ranging from 30·0 to 35·0 (Fig. 2), and agrees with a preferential crystal growing parallel to the helicoidal channel of the apatitic structure. According to this, the relative variation in the intensities of the (300) and (211) diffraction lines, can be tentatively considered as a good approximation for measuring the corresponding variations in the $z/x$ aspect ratio of the microcrystalline particles. Good reproducibility is obtained in the relative intensities from oriented aggregate films, this procedure being used for the diffractograms shown in the next figures. The IR spectrum is given in Fig. 3(a), and shows the absorption bands characteristic for

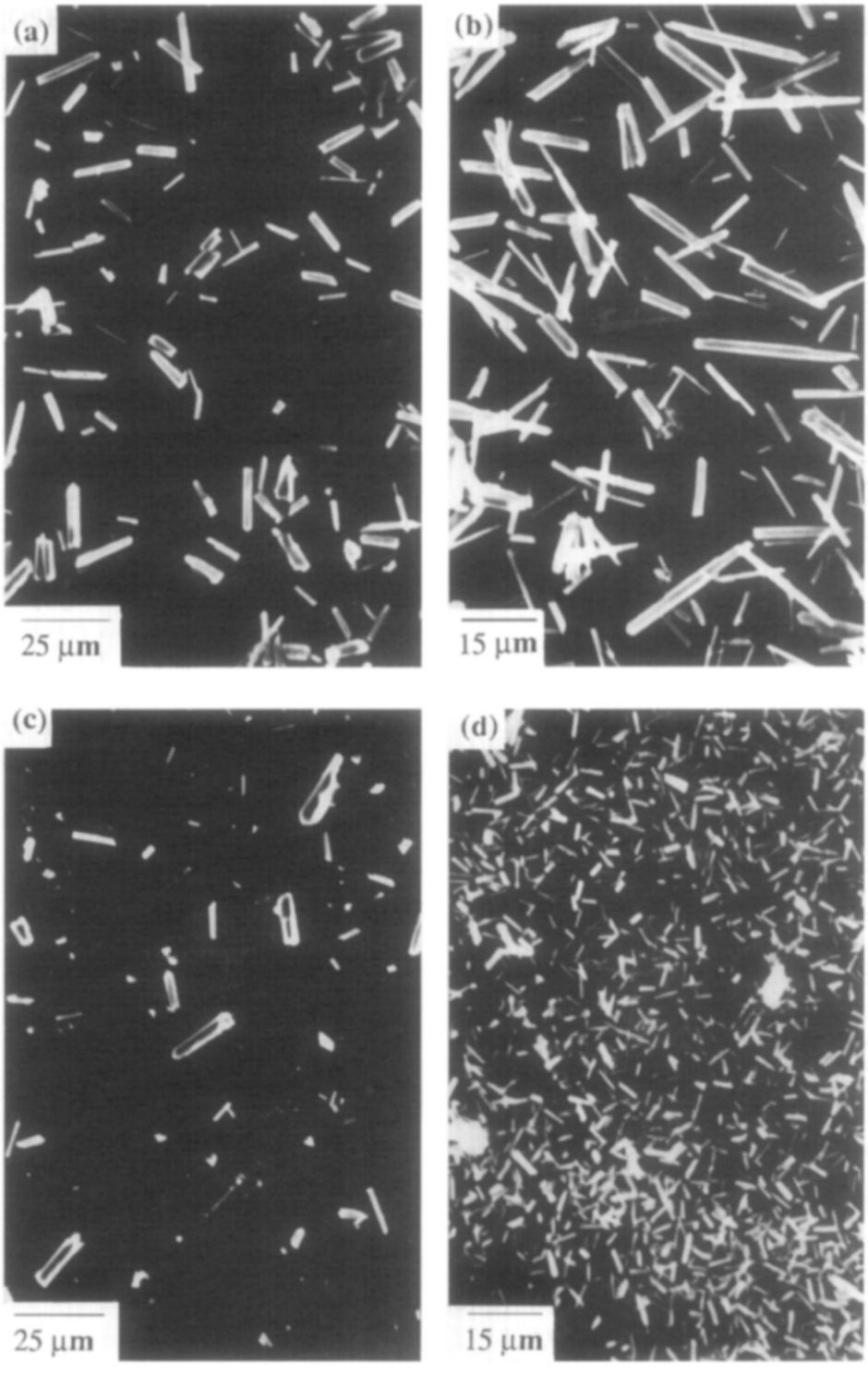


**Fig. 1.** SEM of calcium hydroxyapatites obtained from $Ca(NO_3)_2$ 0·05 M, pH = 11 and $R = 1$ at several temperatures and aging times: (a) 185°C, 1 h; (b) 200°C, 1 h; (c) 220°C, 1 h; (d) 220°C, 24 h.

calcium hydroxyapatite, largely reported in the literature.[22,23] So, the stretching and librational modes of the $OH^-$ groups appear at: $\nu_s$ (3570 $cm^1$), and $\nu_L$ (632 $cm^{-1}$), whereas the internal modes corresponding to the $PO_4^{3-}$ groups occur at: $\nu_3$ (1092, 1048 and 1028 $cm^{-1}$), $\nu_1$ (962 $cm^{-1}$), $\nu_4$ (602, 580 and 564 $cm^{-1}$) and $\nu_2$ (476 and 462 $cm^{-1}$). Also, one additional band of low intensity centered around 840 $cm^{-1}$ can be observed. $CO_3^{2-}$ (type B) or $PO_4H^{2-}$ groups could be responsible for this band.[21,24] However, in both cases, the band appears at ~870 $cm^{-1}$. On the other hand, $CO_3^{2-}$type B presents typical bands in the region 1500–1400 $cm^{-1}$, which are not observed in our case. So, only the $HPO_4^{2-}$ groups appear to be responsible for the band. In order to confirm the origin of this vibration mode, the hydroxyapatite was heated at several temperatures between 250 and 550°C and the corresponding IR spectra were recorded (Fig. 3(b) and (c)). In these conditions, the condensation process $2HPO_4^{2-} = P_2O_7^{4-}$ takes place and a decrease in the intensity of the $HPO_4^{2-}$

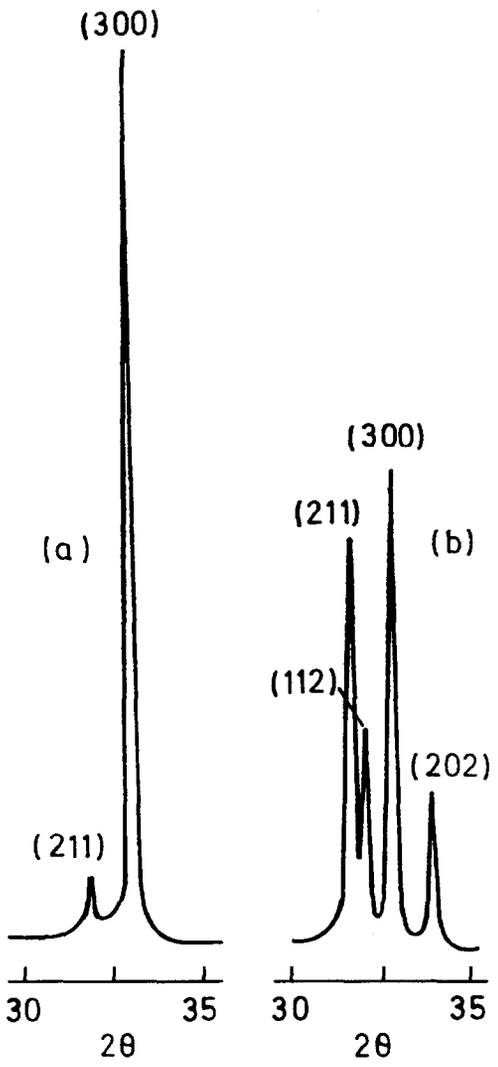


Fig. 2. XRD patterns of calcium hydroxyapatites obtained from $Ca(NO_3)_2$ 0·05 M, pH = 11, $R = 1$, 200°C and aging time 1 h. (a) Oriented aggregate films, (b) non-oriented.

band, which extends over the range 870–840 $cm^{-1}$ together with the presence of a new band at 715 $cm^{-1}$ assignable to pyrophosphate groups are observed.[21] Therefore, the original band at 840 $cm^{-1}$ can be tentatively assigned to $HPO_4^{2-}$ groups. The experimental Ca/P ratio found 1·63, is close to the value corresponding to the HA 1·67, which agrees with the low intensity of the $HPO_4^{2-}$ band. However, the reason for the low frequency of this band still remains unclear. Variations in the lattice parameters can not be claimed because hydroxyapatites synthesised at lower pH (8–9), have very close lattice parameters with respect to the one obtained at pH = 11 and, however, the band appears centered around 870 $cm^{-1}$, in agreement with data reported in the literature.

A tentative explanation could be related with the type of crystalline growing which is shown in the Fig. 4. It can be observed that many particles present an inter-growing shared from (h00) faces. It is plausible to think, that this process could be carried out from the hydrogen bonding interactions between $HPO_4^{2-}$ and /or $HPO_4^{2-}PO_4^{3-}$ groups placed on these faces, which should result in an increase of the P – O distance and therefore in a shifting of the $HPO_4^{2-}$ frequency at lower values. However, additional data are necessary in order to confirm this proposed mechanism.

Considering the eqns (1) and (2), two experiments were carried out in order to obtain hydroxyapatites with higher Ca/P ratio. In one of them, higher concentrations of $Ca^{2+}$ than that of the standard system were allowed by increasing the temperature to 220°C. The aging time was increased to 24 h for reaching nearer conditions to those of the equilibrium. The Ca/P ratio obtained was slightly higher (1·65) and the size of the elongated particles resulted were 2–3 times lower than that obtained in the standard system [Fig. 1(d)]. If it is assumed that in the conditions of the system the solubility of the hydroxyapatites increases as the temperature rises, this result can be explained considering the relation between the critical size ($r^*$) and the relative supersaturation of the solute ($S$), given by: $r* = 2\gamma/[kT/V]\ln S$,[25] where $\gamma$ is the interfacial tension, $V$ is the volume of the precipitating phase and $S$ is the relative supersaturation of the solid. The second experiment was carried out by increasing the pH of the standard system up to 11·8. However, as was previously indicated, $R$ was increased to 1·1 to prevent the formation of precipitate. Contrary to the expected, the Ca/P ratio was lowered to 1·61, indicating that stoichiometric hydroxyapatites can not be obtained

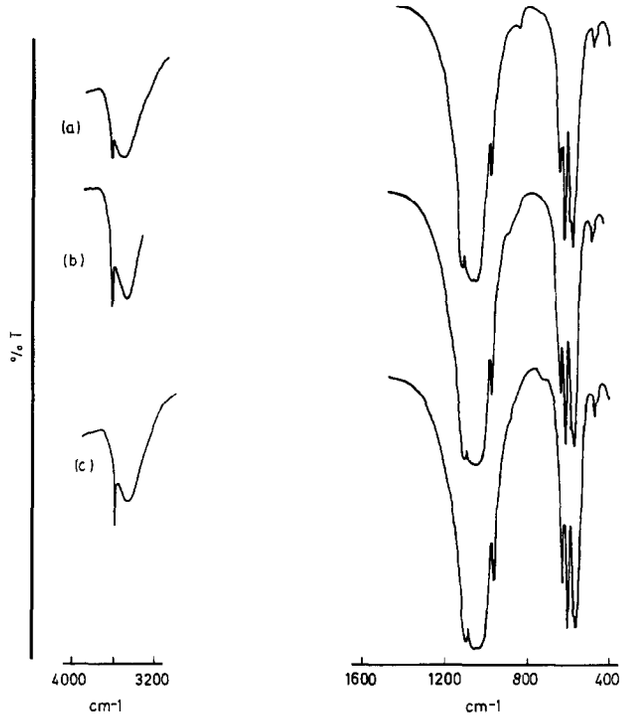


Fig. 3. (a) IR absorption spectra of calcium hydroxyapatite obtained from $Ca(NO_3)_2$ 0·05 M, $R = 1$, 200°C and aging time 1 h; (b) heated at 250°C, 24 h; (c) heated at 500°C, 4 h.

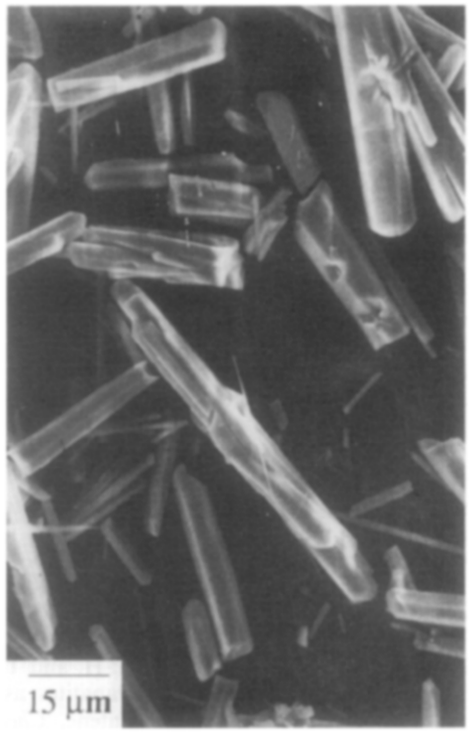


**Fig. 4.** SEM of calcium hydroxyapatites obtained as in Fig. 1(b).

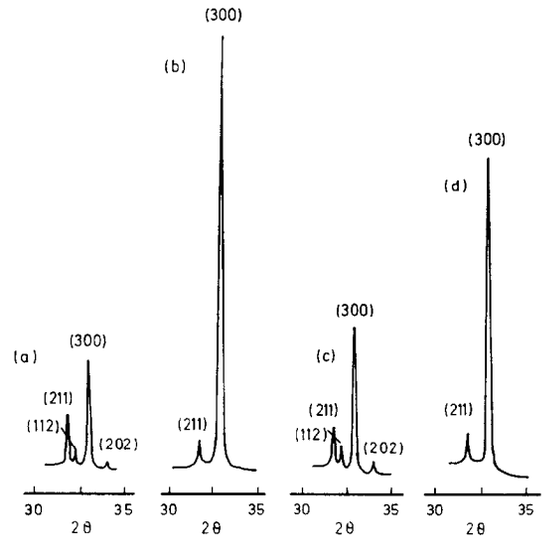


**Fig. 5.** XRD patterns of calcium hydroxyapatites obtained from $Ca(NO_3)_2$ 0·05 M, pH = 11 and aging time 1 h for: (a) 150°C, $R = 1$; (b) 200°C, $R = 1$; (c) 220°C, $R = 1$; (d) 220°C, $R = 1{\cdot}5$.

from this system under these mild hydrothermal conditions. This result is contrary to that reported by Fujishiro *et al.*[8] which affirm that stoichiometric hydroxyapatites are obtained from pH higher than 6.

### 3.2 Influence of temperature and reactant concentrations

With the aim of study being the influence of the reactant concentrations on the morphology and stoichiometric degree, two series of experiments were carried out for $R = 1$ and 1·5, respectively. For $R = 1$, the concentration of calcium nitrate was varied from 0·01 to 0·3 M and for $R = 1{\cdot}5$ between 0·05 and 0·3 M because for calcium nitrate concentrations lower than 0·05 M no precipitate appeared. The temperature was fixed to 200°C. The influence of the temperature was studied for $R = 1$ (150–220°C) and $R = 1{\cdot}5$ (185–220°C), being the concentration of calcium nitrate fixed to 0·05 M. For temperatures lower than 185°C, no precipitate appeared.

It can be said, that the effect of both variables follow a similar trend represented by the temperature in Figs 1 and 5. As the concentration of $Ca^{2+}$ rises from 0·01 up to 0·05 M and the temperature increases from 150 to 200°C, more elongated particles are obtained [Fig. 5(a) and (b)]. For the better conditions: $Ca(NO_3)_2 = 0{\cdot}05$M, 200°C, $R = 1$, the $z/x$ aspect ratio corresponding to the microcrystalline particles can reach values as high as ~60, in contrast to the value lower than the one that presented the non-homogeneous hydroxyapatites. The needle-like microcrystals obtained from such conditions present an average size of 6–18 μm; 1–2·5 μm. This high size variation is related to the hydrothermal process followed. From the lowest temperatures at which the metal complex is dissociated, the $Ca^{2+}$ ions are slowly and continuously liberated in the solution; when the successive sobresaturations are exceeded, progressive nucleations of the solid take place. For

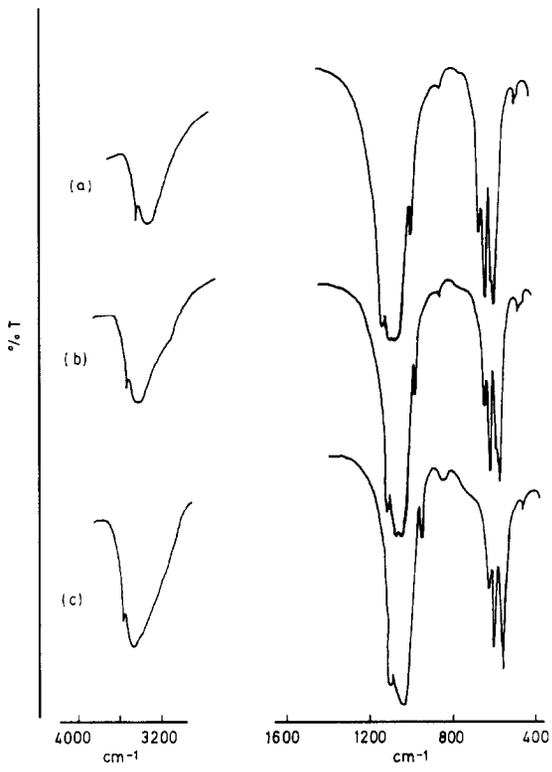


**Fig. 6.** IR absorption spectra of calcium hydroxyapatites obtained from $Ca(NO_3)_2$ 0·05 M, $R = 1$, 200°C and aging time 1 h for: (a) pH = 11; (b) pH = 10; (c) pH = 8.

concentrations of $Ca^{2+}$ higher than 0·05 M and temperatures above 200°C, less developed particles were obtained [Fig. 5(c)]. However, when the last conditions are fixed for $R = 1·5$ higher $z/x$ values are again obtained. The similar trend observed in this process for the effect of the concentration of $Ca^{2+}$ and temperature can be easily understood because both variables are partially interdependent, as can be seen from eqns (1) and (2). The IR spectra are very similar in all cases and only slight differences were found for the Ca/P ratio being near to 1·63.

### 3.3 Effect of pH

Dramatic changes have been observed in both, elongated morphology and stoichiometric degree when the pH was varied. The trend observed in the XRD patterns for pH = 8–11 were similar to that shown in the Fig. 5(a) and (b). The characteristic IR band of the $HPO_4^{2-}$ increases and $\nu_s(OH)$ decreases continuously as the pH decreases (Fig. 6), which agrees well with the non-stoichiometric degree of the samples ranging from 1·63 for pH = 11 to 1·45 for pH = 8. Therefore, it is possible to synthesise homogeneous hydroxyapatites with high differences in the content of $HPO_4^{2-}$ ions. According with this, it is plausible to expect appreciable differences in ionic conductivity for this type of compound.

## References


1. Collins, R. L., Strontium-calcium hydroxyapatite solid-solutions preparation and lattice constants measurements. *J. Am. Chem. Soc.*, 1960, **82**, 89–103.
2. Hayek, E. and Newesely, H., Pentacalcium monohydroxyortophosphate. *Inorg. Synth.*, 1963, **7**, 63.
3. LeGeros, R. Z., Taheri, M. H., Quirolgico, G. and LeGeros, R. P., Formation and stability of apatites: effects of some cationic substituents. *Proc. 2nd Int. Congr. on Phosphorus Compounds*, Boston, 1980, 89–103
4. Andrés-Vergés, M., Higes-Rolando, F. J., Valenzuela-Calahorro, C. and González-Díaz, P. F., On the structure of calcium lead phosphate apatites. *Spectrochim. Acta*, 1983, **39A**(12), 1077–1082.
5. Klein, E., LeGeros, R. P., Trautz, O. R. and LeGeros, R. Z., Polarized infrared reflectance of single crystals of apatites. *Dev. Appl. Spectrosc.*, 1970, **7B**, 3–12.
6. Hattori, T., Iwadate, Y. and Kato, T., Hydrothermal synthesis of hydroxyapatite from calcium acetate and triethyl phosphate. *Advanced Ceramic Materials*, 1998, **3**(4), 427–428.
7. Hattori, T. and Iwadate, Y., Hydrothermal preparation of calcium hydroxyapatite powders. *J. Am. Ceram. Soc.*, 1990, **73**(6), 1803–1805.
8. Fujishiro, Y., Yabuki, H., Kawamura, K., Sato, T. and Okuwaki, A., Preparation of needle-like hydroxyapatite by homogeneous precipitation under hydrothermal conditions. *J. Chem. Tech. Biotechnol.*, 1993, **57**, 349–353.
9. Matsuda, K., Kaneko, Y., Fei, H. J., Fujita, K. and Mitsuzawa, S., Synthesis of hydroxyapatite by hydrolysis of urea. *Pro. Fac. Sci. Tokai Univ.*, 1992, **27**, 73–80.
10. Fowler, B. O., Infrared studies of apatites. II. Preparation of normal and isotopically substituted calcium, strontium and barium hydroxyapatites and spectra-structure composition correlations. *Inorg. Chem.*, 1974, **13**, 207–214.
11. Yamashita, K., Arashi, T., Kitagaki, K., Yamada, S. and Umegaki, T., Preparation of apatite thin films through *rf*-sputtering from calcium phosphate glasses. *J. Am. Ceram. Soc.*, 1994, **77**(9), 2401–2407.
12. Tomsia, A. P., Moya, J. S. and Guitian, F., New route for hydroxyapatite coatings on Ti-based human implants. *Scripta Metallurgica et Materialia*, 1994, **31**, 95–1000.
13. Bett, J. A. S., Christner, L. G. and Hall, W. K., Infrared studies of hydroxyapatite catalists. *J. Catal.* 1969, 332–336.
14. Imizu, Y., Kadoya, M., Abe, H., Itoh, H. and Tada, A., High temperature evacuated hydroxyapatites as a base catalyst for the isomerization of 1-Butene. *Chem. Lett.* 1982, 415–416.
15. Suzuki, T., Hatsushika, T. and Hayakawa, Y., Synthetic hydroxyapatites employed as inorganic cation exchangers I. *J. Chem. Soc., Faraday Trans. 1*, 1981, **77**, 1059–1062.
16. Suzuki, T., Hatsushica, T. and Miyake, M., Synthetic hydroxyapatites employed as inorganic cation exchangers. II. *J. Chem., Soc., Faraday Trans. 1*, 1982, **78**, 3605–3611.
17. Nagai, M., Nishino, T. and Saeki, T., A new type of carbon dioxide gas sensor comprising porous hydroxyapatite ceramics. *Sens. Actuators*, 1988, **15**(2), 145–151.
18. Yamashita, K., Owada, H., Umegaki, T., Kanazawa, T. and Futagami, T., Ionic conduction in apatite solid solutions. *Solid State Ionics*, 1988, **28–30**, 660–663.
19. Yamashita, K., Kitagaki, K. and Umegaki, T., Thermal instability and proton conductivity of ceramic hydroxyapatite at high temperatures. *J. Am. Ceram. Soc.*, 1995, **78**(5), 1191–1197.
20. Chandra, S., *Proton conductors in superionic solids and solid electrolytes*, ed. A. Laskar and S. Chandra. Academic Press, Boston, 1990, pp. 185–226.
21. Joris, S. J. and Amberg, C. H., The nature of deficiency in nonstoichiometric hydroxyapatites. II. Spectroscopic studies of calcium and strontium hydroxyapatites. *J. Phys. Chem.*, 1971, **75**(20), 3172–3178.
22. Baddiel, C. B. and Berry, E. E., Spectra structure correlations in hydroxy and fluorapatite. *Spectrochim. Acta*, 1966, **22**, 1407–1416.
23. Fowler, B. O., Infrared studies of apatites. I. Vibrational assignments for calcium, strontium, and barium hydroxyapatites utilizing isotopic substitution. *Inorg. Chem.*, 1974, **13**, 207–214 .
24. Labarthe, J. C., Bonel, G. and Montel, G., Sur la structure et les propriétés des apatites carbonatées de type B phospho-calciques. *Ann. Chim.*, 1973, **8**, 289–301.
25. Nalbridge, D. J., *Solid/Liquid Dispersions*. Tadros, Th.F., Dubl., Academic Press, 1987.